GIS/Spatial Analyses in Fishery and Aquatic Sciences (Vol.4)
(7) Corbineau et al – Spatial & temporal patterns of Japan tuna longline fisheries (tropical waters) (097-114)

Analysis of the spatial and temporal patterns of Japanese tuna longline fisheries in the tropical world ocean

Ana Corbineau
IRD, UMR 212 EME,
Centre de Recherche Halieutique Méditerranéenne et Tropicale,
Avenue Jean Monnet, BP 171, 34203 Sète cedex, France

Tristan Rouyer
Jean-Marc Fromentin
IFREMER, Centre de Recherche Halieutique,
Méditerranéenne et Tropicale
Avenue Jean Monnet, BP 171, 34203 Sète cedex, France

Bernard Cazelles
CNRS UMR 7625, ENS, 46 rue d'Ulm, 75230 Paris Cedex 05, France
and
UR 079 GEODES, Centre IRD Ile de France
32 avenue Henri Varagnat, 93142 Bondy cedex, France

Alain Fonteneau
IRD, UMR 212 EME, Centre de Recherche Halieutique
Méditerranéenne et Tropicale
Avenue Jean Monnet, BP 171, 34203 Sète cedex, France

Frédéric Ménard*
Institut de Recherche pour le Développement, UMR 212 EME,
Centre de Recherche Halieutique Méditerranéenne et Tropicale,
Avenue Jean Monnet, BP 171, 34203 Sète cedex-France
Phone: 33 (France) 4 99 57 32 30
Fax: 33 (France) 4 99 57 32 95
E-mail: Frederic.Menard@ird.fr

---

* *Corresponding author*

Abstract

The industrial-tuna-fishery development in the world ocean since the early 1950s and its reliable documentation by the Tuna Commission allow us to extract data from the mainly-exploited species with contrasting life-story traits and to construct catch and catch-rate (CPUE) time series. We used the biogeographic provinces of Longhurst to extract the fishery data for the three oceanic basins, and we selected four main species (yellowfin and bigeye tunas, swordfish and blue marlin) exploited by the Japanese tuna longliners from 1960 to 2004. In order to study patterns of variability that characterize catch and CPUE time series we used Wavelet Analysis and then, basing on the Maximum Covariance Analysis between each pair of wavelet spectra, we performed a multivariate analysis to classify the time series and to identify the influent factor (species, province or ocean). Finally, we studied relationships between catch and CPUE time-series and large-climate indices, carrying out Cross Wavelet Analysis. This comparative approach mixing data for different tuna and tuna-like species in several areas of the tropical world ocean provides a powerful way to identify the fundamental factors associated with population fluctuations. Our results show that the spatial scale of the bigeographic provinces of Longhurst appears to be one of the most important factors to take into account when analyzing longline-fisheries data. In addition, this study also demonstrates the potential impact of large-scale climate variability, and confirmed that CPUE data poorly reflect the underlying processes that drive the fluctuation in abundance of large pelagic fish.

Key words

biogeographic provinces, pelagic fishes, time-series analysis, tuna, wavelet analysis.

1. Introduction

In general, the functioning of marine ecosystems depends on the interactions between species, populations and environment, and several external factors have an essential role on the dynamics of these populations (Covich *et al.*, 2004). Exploited marine fish stocks fluctuate over a large range of spatial and temporal scales, exhibiting variability on seasonal, interannual, and/or decadal scales (Castro-Ortiz and Lluch-Belda, 2007; Ravier and Fromentin, 2004; Cushing and Dickson, 1976). Fisheries variability is known to be related to changes in their environment that affect distribution, migration, and abundance of fish resources (Glantz, 1992). Indeed, environmental variability affects biological mechanisms of a fish population's dynamics as well as fish availability, fleet dynamics and catchability of targeted species (Stenseth *et al.*, 2004). The temporal patterns that may govern the variability of exploited fish can be identified by analysing long time-series of commercial catches. Time-series analyses can reveal a substantial amount of information on the temporal and spatial dynamics of these exploited ecosystems by improving knowledge on the association between environmental variability and fish fluctuations. Local environmental conditions play an important role on fish habitat and are very often associated with large-scale climate indices such as the North Atlantic Oscillation in the Atlantic Ocean (Rouyer *et al.*, 2008a), the Indian Oscillation Index or the Dipole Mode Index in the Indian Ocean (Ménard *et al.*, 2007; Corbineau *et al.*, 2008), or the ENSO cycles in the Pacific Ocean (Lehodey *et al.*, 1997, 2003).

It is in this context that we intend to analyse the patterns of variations of four tunas and tuna-like species in the biogeographic provinces of Longhurst (1998) of the tropical world ocean (Indian, Atlantic and Pacific Oceans). Our approach was already conducted in the Atlantic and Indian Oceans (Corbineau *et al.*, 2010), but to the best of our knowledge, this is the first analysis carried out in the three oceans. We worked here with extensive statistics from the Japanese longline fisheries. The four selected fish species are pelagic top predators (two tuna species, swordfish and blue marlin) that exhibit different fishing pressure. The time-scale pattern for each yearly time series extracted by sub area was determined using wavelet analyses (Cazelles *et al.*, 2008). Cluster analysis allowed us to identify groups with similar patterns of variability according to their wavelet spectra (Rouyer *et al.*, 2008b). We also investigate the relationships between tuna time-series and the Southern Oscillation Index (SOI) using the same methodological approach.

2. Material and methods

2.1. Fishery data

Catch and effort data of the Japanese industrial longline fishery are available since the 1950s, by 5° square and by month from the Indian Ocean Tuna Commission (IOTC, *http://www.iotc.org*) data base, from the International Commission for the Conservation of Atlantic tunas (ICCAT, *http://www.iccat.int*), from the Western and Central Pacific Fisheries Commission (*WCPFC, http://www.wcpfc.int*), and from the Inter-American Tropical Tuna Commission (IATTC, *http://iattc.org*) for the Eastern Pacific. Time series of catch and catch per unit of effort (CPUE) have been extracted within the Longhurst provinces (Longhurst, 1998; Figure 1) with respect to the same time period in the three oceans (from 1960 to 2004).

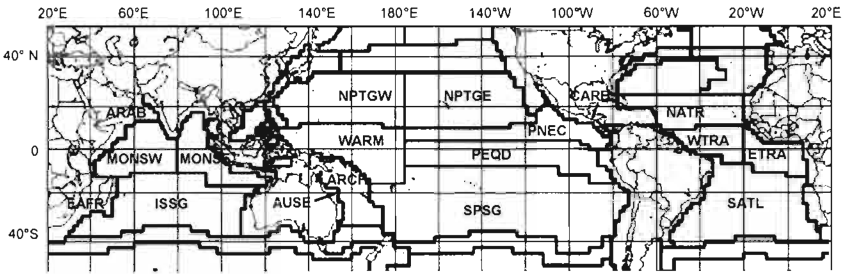

Figure 1. The biogeographic provinces of Longhurst (adapted from Longhurst, 1998). Legend: ARAB: Northwestern Arabian Upwelling province; MONSW: Indian Monsoon Gyres Western province; MONSE: Indian Monsoon Gyres Eastern province; EAFR: Eastern Africa Coastal province; ISSG: Indian South Subtropical Gyre province; NATR: North Atlantic Tropical Gyral province; CARB: Caribbean province; WTRA: Western Tropical Atlantic province; ETRA: Eastern Tropical Atlantic province; SATL: South Atlantic Gyral province; SPSG: South Pacific Subtropical Gyre province; ARCH: Archipelagic Deep Basins province; AUSE: Eastern Australian Coastal province; WARM: Western Pacific Warm Pool Province; PEQD: Pacific Equatorial Divergence province; PNEC: North Pacific Equatorial Counter-current province; NPTGE: North Pacific Tropical Gyre Eastern province; and NPTGW: North Pacific Tropical Gyre Western province.

The time series from five provinces were analyzed in the Indian Ocean:

- *the Indian South Subtropical Gyre province (ISSG);*
- *the Eastern Africa Coastal province (EAFR);*
- *the Northwest Arabian Upwelling province (ARAB); and*
- *the original Indian Monsoon Gyres province of Longhurst was for convenience divided into a West sub-province (MONSW) and an East sub-province (MONSE) according to the spatial patterns of environmental variables characterizing the Indian Ocean Dipole (Saji et al., 1999; Corbineau et al., 2008).*

In the tropical Atlantic Ocean, we selected five additional provinces:

- *the North Atlantic Tropical Gyral province (NATR);*
- *the Caribbean province (CARB);*
- *the Western Tropical Atlantic province (WTRA);*
- *the Eastern Tropical Atlantic province (ETRA); and*
- *the South Atlantic Gyral province (SATL).*

According to their small sizes and their closeness to the African coast, data from the Eastern Canary Coastal province (CNRY) and the Guinea Current Coastal province (GUIN) were compiled with the NATR and ETRA provinces, respectively.

In the tropical Pacific, we took into account eight extra provinces:

- *the South Pacific Subtropical Gyre province (SPSG);*
- *the Archipelagic Deep Basins province (ARCH);*
- *the East Australian Coastal province (AUSE);*
- *the Western Pacific Warm Pool province (WARM);*
- *the Pacific Equatorial Divergence province (PEQD);*
- *the North Pacific Equatorial Counter-current province (PNEC); and*
- *the North Pacific Tropical Gyre province (NPTG). For convenience, the last one was divided into East (NPTGE) and West (NPTGW) sub-provinces according to the spatial patterns typifying some species dominance (The NPTG province is well typified by albacore dominance, but this is clearer in their western than in their eastern parts, supporting the separation of NPTG into E and W provinces; A. Longhurst, pers. comm.)*

Acronyms for the provinces are given in Table 1.

Table 1. Longhurst provinces used, and associated acronyms.

Province	Acronym
Indian Ocean	
Northwestern Arabian Upwelling province	ARAB
Indian Monsoon Gyres Western province	MONSW
Indian Monsoon Gyres Eastern province	MONSE
Eastern Africa Coastal province	EAFR
Indian South Subtropical Gyre province	ISSG
Atlantic Ocean	
North Atlantic Tropical Gyral province	NATR
Caribbean province	CARB
Western Tropical Atlantic province	WTRA
Eastern Tropical Atlantic province	ETRA
South Atlantic Gyral province	SATL
Pacific Ocean	
North Pacific Tropical Gyre Western province	NPTGW
North Pacific Tropical Gyre Eastern province	NPTGE
Western Pacific Warm Pool province	WARM
North Pacific Equatorial Counter-current province	PNEC
Pacific Equatorial Divergence province	PEQD
South Pacific Subtropical Gyre province	SPSG
Archipelagic Deep Basins province	ARCH
Eastern Australian Coastal province	AUSE
South Pacific Subtropical Gyre province	SPSG

In each province, we extracted the time series of catch and CPUE for yellowfin tuna (*Thunnus albacares*; YFT hereafter), bigeye tuna (*Thunnus obesus*; BET hereafter), swordfish (*Xiphias gladius*; SWO hereafter), and blue marlin (*Makaira mazara* in the Indian and Pacific Oceans and *M. nigricans* in the Atlantic Ocean; BUM hereafter) (Acronyms are given in Table 2). Nominal CPUE were computed by averaging ratios of catch in number to the number of hooks. Several time series were not informative and were discarded from the analyses. We obtained 66 catch time-series and 66 CPUE time-series characterized by three factors: the species (4 modalities), the provinces (18 modalities) and the ocean (3 modalities).

Table 2. Common name, scientific name and code used for the species.

Common name	Scientific name	Code
Yellowfin	*Thunnus albacares*	YFT
Bigeye	*Thunnus obesus*	BET
Swordfish	*Xiphias gladius*	SWO
Blue marlin	*Makaira nigricans* *(Atlantic ocean)* *Makaira mazara* *(Indian and Pacific Oceans)*	BUM

2.2 Climatic index

The Southern Oscillation Index (SOI) is considered as the main climate index that most likely impacts the world ocean (Stenseth *et al.*, 2003). The SOI provides a measure of the large-scale fluctuations in air pressure occurring between the western and eastern tropical Pacific (Trenberth, 1997). The monthly SOI index was averaged to calculate a yearly time-series. The SOI strongly fluctuates (Trenberth, 1984), but has two major oscillation periods of 4~6 years and of 10~14 years, respectively.

2.3 Time-series analysis

The wavelet analysis performs a time-scale decomposition of the signal, highlighting the periodic components of each time series and detecting relationships between two signals, taking into account the complexity, the irregularity and the non-stationarity of the series (Cazelles *et al.*, 2008; Torrence and Campo, 1998).

This method application allows calculation of the wavelet power spectrum (WPS) that gives a measurement of the distribution of the variance to each time for the studied series (Ménard *et al.*, 2007). The WPS can be represented by a plot with two dimensions where the time is represented on the *x*-axis and the period (frequency) on the *y*-axis.

To determine relations between two signals, we carried out wavelet cross-spectrum (WCS) examination. Consequently, the WCS gives a measurement of the covariance between the spectra of two time series. The WCS is also represented graphically, like the WPS.

Once the wavelet analyses were performed, the 66 WPSs were grouped according to a multivariate analysis involving a clustering method. We carried out the same approach to compare the WCSs between the 66 biological time series and the SOI. In addition, we plotted the distances originated from the cluster using boxplots in order to investigate the main effects. The method is fully described in Rouyer *et al.* (2008b), and the Appendix gives supplementary information.

3. Results

3.1 Variability patterns of the catch time-series

The cluster analysis classified the wavelet spectra of the 66 time series into 10 groups (Figure 2, left). YFT and BUM of the three oceans are the principal species of the first group (G_1). The second (G_2) grouped several time series from the Pacific only, as well as the third group (G_3) with a dominance of North provinces (NPTGW and NPTGE); all species occurred here in close proportions. The fourth (G_4) is dominated by Atlantic provinces. Conversely, Pacific provinces prevailed in group G_5. Group G_6 put together several Atlantic and Pacific provinces. Three PEQD provinces of the Pacific and three ARAB provinces of the Indian are grouped in G_7 and G_8, respectively. Group G_9 is dominated by Indian provinces, with BET the major species. The last group (G_{10}) is dominated by YFT from Pacific and Atlantic provinces in close proportions. Thus the dendrogram of the dissimilarities between the WPSs evidenced a clear grouping by province and ocean rather than by species. The boxplots of Figure 3 display the distributions of the dissimilarities among the factors and the modalities: Figure 3a confirms that the province factor has the most structuring effect; in addition, the time series of the Indian Ocean have the highest similarity among the three oceans. Figure 3b ("species modalities") shows no clear pattern from the species modalities.

3.2 Catch time-series and climate variability

A new dendrogram was performed based on the dissimilarities of the 66 WCSs characterizing the associations between the SOI and the tuna catch time-series. This new dendrogram (Figure 2, right) exhibits more structure than the previous one (Figure 2, left): eight groups were identified, and the median of the WCS dissimilarities was 16% less than the median of the WPS dissimilarities (Figure 2, left). The boxplots of the dissimilarities among the factors (Figure 3d) show the same patterns described in the previous section.

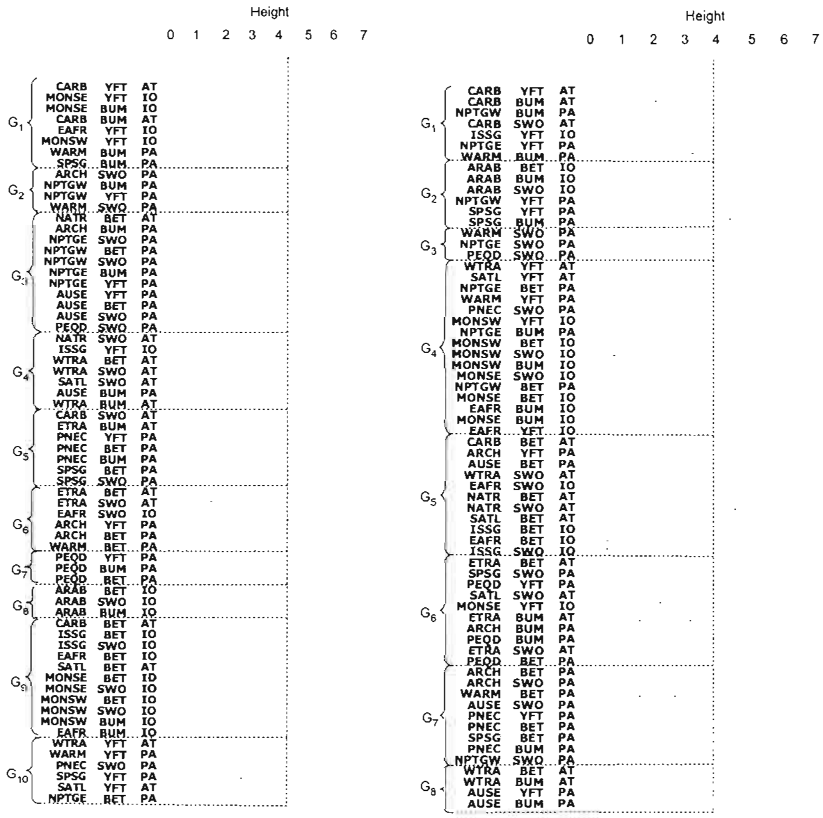

Figure 2. Left: Cluster dendrogram of the wavelet power spectra of the 66 catch time-series. Right: Cluster dendrogram of the wavelet cross-spectra between the 66 catch time-series and the Southern Oscillation Index. Time period: 1960–2004. The dashed line discriminates the groups (G_1– G_{10}). The height represents the level of dissimilarity between the distances of each pair of wavelet spectra. Acronyms for provinces are given in Table 1 and for species are given in Table 2. AT = Atlantic Ocean; IO = Indian Ocean; and PA = Pacific Ocean.

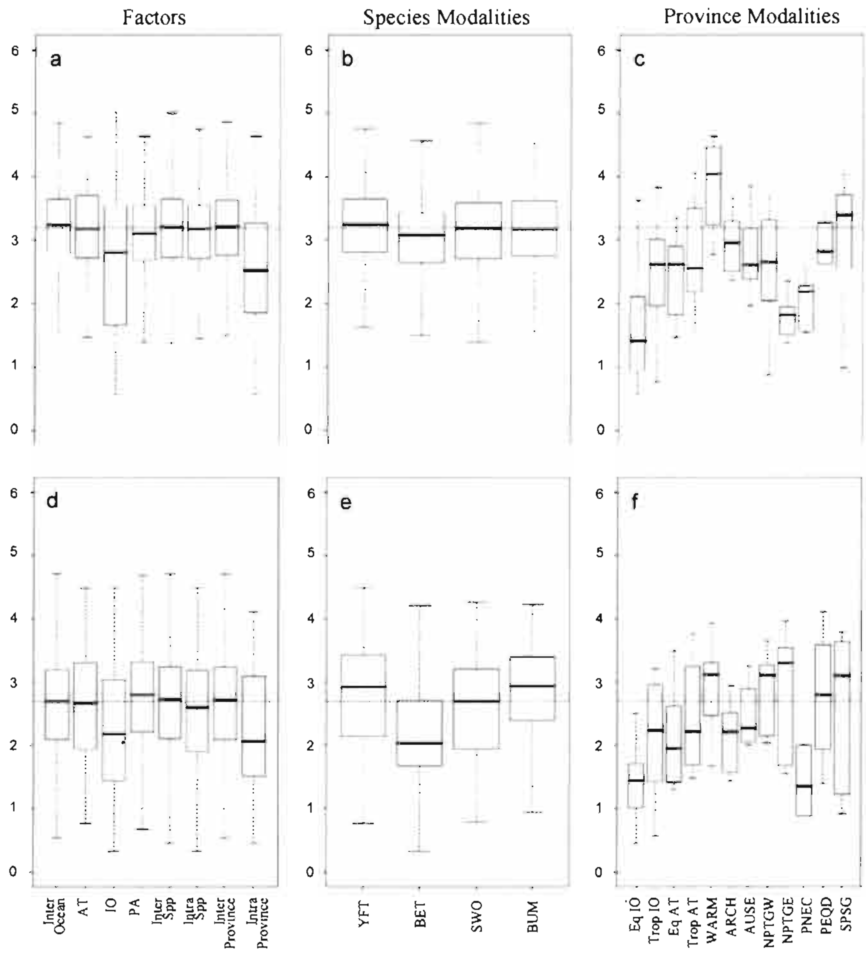

Figure 3. Boxplots of the dissimilarities of sub-sets extracted. Boxplots by factors (a), by species modalities (b), and by province modalities (c) from the wavelet power spectra of the catch time-series. Boxplots by factor (d), by species modalities (e), and by province modalities (f) from the wavelet cross-spectra between the catch time-series and the SOI signal. The y-axis values represent the dissimilarities of sub-sets extracted from the distance matrix. The horizontal dotted line represents the general median calculated from the distance matrix which contains the dissimilarities between all pairs of wavelet spectra. Legend: AT = Atlantic Ocean; IO = Indian Ocean; PA = Pacific Ocean; Eq IO = Equatorial Indian Ocean (ARAB, MONSW and MONSE provinces); Trop IO = Tropical Indian Ocean (EAFR and ISSG provinces); Eq AT = Equatorial Atlantic Ocean (WTRA and ETRA provinces); and Trop AT = Atlantic Ocean tropical provinces (NATR, SATL and CARB provinces). Acronyms for provinces are given in Table 1 and for species are given in Table 2.

However, the boxplots by species modalities (Figure 3e) indicates that the cross with the SOI bring closer the patterns of variation of the bigeye tuna time series only. Among provinces, the equatorial Indian Ocean (i.e., the MONSW, MONSE and ARAB provinces) has a greater homogeneity when tuna time-series were associated with the SOI. Similarly, the gyre (NATR and SATL) and equatorial (WTRA and ETRA) provinces of the Atlantic Ocean exhibit a decrease of their medians compared to the boxplots of Figure 3c. In the Pacific Ocean, the medians of the WARM, ARCH and AUSE provinces also decrease by 22.7%, 25.3% and 13.1%, respectively. The medians of the SPSG and PEQD provinces remain quite stable (decrease of 8.8% and 0.7%, respectively), while their first and third quartiles considerably increase. On one hand, the median of the PNEC province decreases by 38% and on the other hand, the medians of the NPTGW and NPTGE provinces increase about 16% and 82%, respectively. Note that the NPTGE boxplot exhibits a very large range of dissimilarities.

3.3 CPUE time series

The same approach was performed with the CPUE data and the SOI signal but results are not shown because no patterns were evident: neither with the dendrograms nor with the boxplots.

4. Discussion

Based on the approach used by Rouyer *et al.* (2008a), Corbineau *et al.* (in press) already showed that the biogeographic provinces of Longhurst (1998) were the most obvious factor that influences the patterns of variation of tunas and tuna-like species in the Indian and Atlantic Oceans. Here, the main purpose of our work was to analyse the data again, but at the global scale of the tropical world ocean, i.e. including the Pacific Ocean that is the biggest oceanic basin and that exhibits the highest levels of tuna exploitation. Extension of this work to the tropical world ocean was achievable because of the recent availability of the Japanese longline datasets for the Pacific Ocean. We were thus able to analyse and compare 66 catch time-series for the Indian, Atlantic, and Pacific Oceans.

Our results confirm that the species is not a key structuring factor to classify the patterns of variation of tuna and tuna-like species. Thus, our results reinforce the role of the spatial scales when analyzing fisheries data from the three oceans. Boxplots by modality showed a great heterogeneity at the province level for each ocean: the Indian Ocean appears to be the most structured ocean with a high homogeneity between the equatorial provinces (ARAB, MONSW, and MONSE), while the tropical provinces (EAFR and ISSG) were grouped with the Atlantic provinces. Contrary to this, the provinces of the Pacific Ocean exhibited great heterogeneity: equatorial or tropical provinces could indeed not be grouped. Nevertheless, we identified similarities between the West provinces (ARCH, AUSE and NPTGW), and between the East provinces (NPTE and PNEC). However, the WARM, PEQD and SPSG provinces could not be included in this East versus West division, because of substantial differences regarding their respective boxplots. In fact, the Pacific Ocean represents a huge surface of the world ocean. It exhibits strong longitudinal differences in mixed-layer depth and in other physical circulation features (Longhurst, 1998). This can explain in part why some East and West provinces are similar to each other. On the other hand, the WARM province is very heterogeneous and significantly different from the others. Indeed the wavelet spectra of the WARM time series are very dissimilar to each other; while the bigeye wavelet power spectrum presents high variability about 2–3 years, the swordfish WPS presents periodic cycles around 4–6 years and the yellowfin WPS in the 12–16-year band (Figure 4). The WARM province is typified by yellowfin tuna and exhibits by far the highest catches among the provinces of the Pacific Ocean and of the other oceans. Our results also reinforce the use of nominal CPUE data as an abundance index in such analysis. The nominal CPUE data from the Japanese longline fishery present several intrinsic biases that preclude their use for providing relevant information on the patterns of variation of tunas and tuna-like species (Polacheck, 2006). Indeed, for fisheries where effort was initially concentrated in a few cells then later spread widely, as in the Japanese pelagic longline fishery, catch rates have typically dropped in the initial fishing areas before fishers were willing to spread their efforts more widely. The catch-rate declines in such areas are not in any way representative of overall stock change (Walters, 2003). Therefore, a local aggregation of fishing vessels in a productive area can generate high catches, high levels of fishing effort, and low catch rates, although these high catches indicate high biomass areas (Gillis and Peterman, 1998). Actually, nominal CPUE data were based on the available hook number by 5° x 5° grid areas and month. This aggregated measure of the fishing effort may generate major uncertainties and cannot take into account the changes in targeting practices, biasing in addition the investigations for by-catch species (Fonteneau and Richard, 2003; Bigelow *et al.*, 2002; Bach *et al.*, 2006; Maunder *et al.*, 2006). In the same way, using this aggregated measure assumes that catchability is constant across species and over the time while fleets improve fishing gears and practices which increase catchability and alter the relationship between catch rates and abundance (Ward and Hindmarsh, 2007).

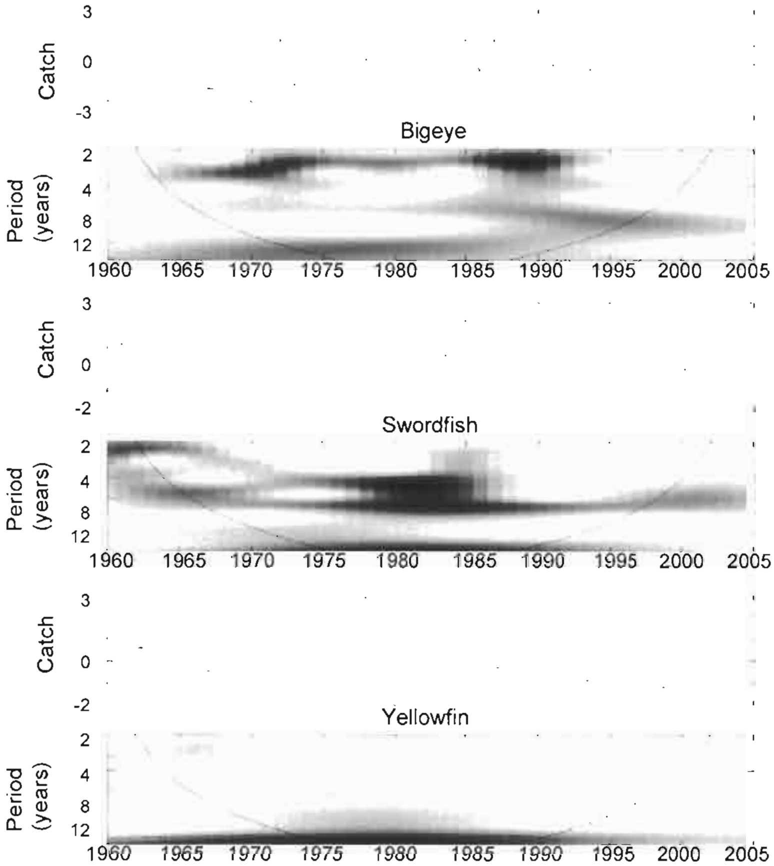

Figure 4. Wavelet analyses of the standardized catch time-series of bigeye, swordfish and yellowfin from 1960 to 2004 in the Western Pacific Warm Pool province. High power values are represented in black and low power values in white. The dotted lines show the 5% significance level. The grey solid lines delimit the cone of influence, i.e., the region where the edge effects are present.

Corbineau *et al.* (2010) have already investigated the role of the SOI in the Indian Ocean and in the Atlantic Ocean. In the Indian Ocean, the main SOI impact was in the equatorial area, while in the Atlantic the influence of the SOI was apparent in the equatorial and tropical areas, especially in the NATR province. The present study added the Pacific Ocean. Our results suggest that large climatic oscillations impacted all the time series but the impact of the SOI was more obvious at the province scale. The SOI dominates the environmental forcing of the Pacific provinces, where ENSO events occur with more intensity than in the other oceans (Lehodey *et al.*, 2006). The low influence of the SOI in AUSE, ARCH and WARM provinces can be explained by their locations in the most western regions of the Pacific basin, i.e. where SOI effects are not salient. On the other hand, our results showed that NPTGW, NPTGE (NPTG) and PNEC are strongly affected by the SOI. In fact, these provinces and the PEQD, located in the eastern part of the Pacific Ocean, lose their oceanographic features partially or completely during an ENSO event (Longhurst, 1998). During an ENSO event, the usual warm waters of the surface layer that characterised the western equatorial Pacific extend to the east in the central Pacific. This extension of the warm pool is concomitant with changes in the ocean–atmosphere circulation with major impacts on the thermocline depth, primary production, trophodynamic relationships and, finally, movements and migration of tuna populations (Lehodey *et al.*, 2006). The NPTGE province had a larger median and a greater heterogeneity of WCS dissimilarities, suggesting that the tunas and tuna-like species did not respond in the same way to ENSO cycles: while relationships between yellowfin tuna and the SOI are evidenced in the 3–4-year band from 1965 to 1975, swordfish and SOI co-varied on the 3–4-year band in the middle of the 1960s and on the 4–6-year band from 1980 to 1985. Variability of bigeye tuna and blue marlin is associated with the SOI in the long term (12–16 years) for the entire studied period, as well as in the short term (3–4 years) from the middle of the 1960s to the end of the 1970s (figures not shown). In the same way, we expected that the SOI signal brought nearer the patterns of variation of the catch time-series of the PEQD province. The lack of apparent homogeneity in this province emphasizes the unpredictable response of species to ENSO events.

This comparative approach conducted in the world ocean highlights the role of spatial scales and geographic locations when analysing fisheries data. Despite the distinctive features of each ocean, the use of time series of different tuna species in the Longhurst's provinces showed the importance of spatial processes in the top predators' distribution. In other words, there is a link between the oceanographic parameters that characterize the provinces (biogeochemical properties of sea water, primary production, nutrient dynamics and mixed-layer depth) and the high trophic levels through propagation along the food chain up to top predators. Thus, changes in oceanographic parameters that regulate abundance of the first trophic levels have repercussions on the whole trophic chain by complex mechanisms of regulations ("bottom up" control).

Acknowledgements

The authors gratefully thank Alan Longhurst. This work, a part of the THETIS programme of the IRD (Institut de Recherche pour le Développement), is also supported by the REMIGE project funded by Agence Nationale de la Recherche (ANR 2005 Biodiv-011). A. Corbineau is supported by a grant from Département Soutien et Formation, Institut de Recherche pour le Développement.

References

Bach, P., Travassos, P.D. and Gaertner, D. 2006. Why the number of hooks per basket (HPB) is not a good proxy indicator of the maximum fishing depth in drifting longline fisheries? Collected Volume of Scientific Papers, ICCAT, 59: 701–715.

Bigelow, K.A., Hampton, J. and Miyabe, N. 2002. Application of a habitat-based model to estimate effective longline fishing effort and relative abundance of Pacific bigeye tuna (*Thunnus obesus*). Fisheries Oceanography, 11: 143–155.

Bretherton, C.S., Smith, C. and Wallace, J.M. 1992. An intercomparison of methods for finding coupled patterns in climate data. Journal of Climatology, 5: 541-560.

Castro-Ortiz, J.L. and Lluch-Belda, D. 2007. Low frequency variability of fishing resources, climate, and ocean. Fisheries Research, 85: 186–196.

Cazelles, B., Chavez, M., Berteaux, D., Ménard, F., Vik J.O., Jenouvrier, S. and Stenseth, N.C. 2008. Wavelet analysis of ecological time series. Oecologia, 156: 287–304.

Corbineau, A., Rouyer, T., Cazelles, B., Fromentin, J-M., Fonteneau, A. and Ménard, F. 2008. Time series analysis of tuna and swordfish catches and climate variability in the Indian Ocean (1968–2003). Aquatic Living Resources, 21: 277–285.

Corbineau, A., Rouyer, T., Cazelles, B., Fromentin, J-M., Fonteneau, A. and Ménard, F. 2010. Patterns of variations in large pelagic fish: a comparative approach between the Indian and Atlantic Oceans. Progress in Oceanography, doi:10.1016/j.pocean.2010.04.019

Covich, A.P., Austen, M.C., Bärlocher, F., Chauvet, E., Cardinale, B.J., Biles, C.L., Inchausti, P., Dangles, O., Solan, M., Gessner, M.O., Statzner, B. and Moss, B. 2004. The role of biodiversity in the functioning of freshwater and marine benthic ecosystems. Bioscience, 54: 767–775.

Cushing, D.H. and Dickson, R.R. 1976. The biological response in the sea to climatic changes. Advances in Marine Biology, 14: 1–122.

Fonteneau, A. and Richard, N. 2003. Relationship between catch, effort, CPUE and local abundance of non-target species, such as billfishes, caught by Indian Ocean longline fisheries. Marine and Freshwater Research, 54: 1–10.

Gillis, D.M. and Peterman, R.M. 1998. Implications of interference among fishing vessels and the ideal free distribution to the interpretation of CPUE. Canadian Journal of Fisheries and Aquatic Sciences, 55: 37–46.

Glantz, M.H. 1992. Climate Variability, Climate Change and Fisheries. Cambridge University Press, Cambridge. 450 pp.

Lehodey, P., Bertignac, M., Hampton, J., Lewis, A. and Picaut, J. 1997. El Niño Southern Oscillation and tuna in the western Pacific. Nature, 389: 715–717.

Lehodey, P., Chai, F. and Hampton, J. 2003. Modelling climate-related variability of tuna populations from a coupled ocean-biogeochemical – population-dynamics model. Fisheries Oceanography, 12: 483–494.

Lehodey, P., Alheit, J., Barange, M., Baumgartner, T., Beaugrand, G., Drinkwater, K., Fromentin J-M., Hare, S.R., Ottersen, G., Perry, R.I., Roy, C., Van der Lingen, C.D. and Werner, F. 2006. Climate variability, fish and fisheries. Journal of Climate, 19: 5009–5030.

Longhurst, A.R. 1998. Ecological Geography of the Sea. Academic Press, San Diego, 398 pp.

Maunder, M.N., Sibert, J.R., Fonteneau, A., Hampton, J., Kleiber, P. and Harley, S.J. 2006. Interpreting catch per unit effort data to assess the status of individual stocks and communities. ICES Journal of Marine Science, 63: 1373–1385.

Ménard, F., Marsac, F., Bellier, E. and Cazelles, B. 2007. Climatic oscillations and tuna catch rates in the Indian Ocean: a wavelet approach of time series analysis. Fisheries Oceanography, 16: 95–104.

Polachek, T. 2006. Tuna longline catch rates in the Indian Ocean: Did industrial fishing result in a 90% rapid decline in the abundance of large predatory species? Marine Policy, 30: 470–482.

Ravier, C. and Fromentin, J.-M. 2004. Are the long-term fluctuations in Atlantic bluefin tuna (*Thunnus thynnus*) population related to environmental changes? Fisheries Oceanography, 13: 145–160.

Rouyer, T., Fromentin, J.-M., Ménard, F., Cazelles, B., Briand, K., Pianet, R., Planque, B. and Stenseth, N.C. 2008a. Complex interplays among population dynamics, environmental forcing and exploitation in fisheries. Proceedings of the National Academy of Sciences, 105: 5420–5425.

Rouyer, T., Fromentin, J.-M., Stenseth, N.C. and Cazelles, B. 2008b. Analysing multiple time series and extending significance testing in wavelet analysis. Marine Ecology Progress Series, 359: 11–23.

Saji, N.H., Goswami, B.N., Vinayachandran, P.N. and Yamagata, T. 1999. A dipole mode in the tropical Indian Ocean. Nature 401: 360–363.

Stenseth, N.C., Ottersen, G., Hurrell, J.W. and Belgrano, A. 2004. Marine Ecosystems and Climate Variation. Oxford University Press Inc., New York. 252 pp.

Stenseth, N.C., Ottersen, G., Hurrell, J.W., Mysterud, A., Lima, M., Chan, K-S., Yoccoz, N.G. and Adlandsvik, B. 2003. Studying climate effects on ecology through the use of climate indices: the North Atlantic Oscillation, El Niño Southern Oscillation and beyond. Proceedings of the Royal Society B, 270: 2087–2096.

Torrence, C. and Campo, G.P. 1998. A practical guide to wavelet analysis. Bulletin of American Meteorology Society, 79: 61–78.

Trenberth, K.E. 1984. Signal versus noise in the Southern Oscillation. Monthly Weather Review, 112: 326–332.

Trenberth, K.E. 1997. The definition of El Niño. Bulletin of the American Meteorological Society, 78: 2771–2777.

Walters, C. 2003. Folly and fantasy in the analysis of spatial catch rate data. Canadian Journal of Fisheries and Aquatic Sciences, 60: 1433–1436.

Ward, P. and Hindmarsh, S. 2007. An overview of historical changes in the fishing gear and practices of pelagic longliners, with particular reference to Japan's Pacific fleet. Reviews in Fish Biology and Fisheries, 17: 501–516.

APPENDIX

Wavelets derive from a mother wavelet ψ(t), expressed as a function of the time position τ and the scale of the wavelets *a*. A wavelet transform of a time series *x(t)* is defined as a convolution product:

$$W_x(a,\tau) = \frac{1}{\sqrt{a}}\int_{-\infty}^{+\infty} x(t)\psi^*\left(\frac{t-\tau}{a}\right)dt$$

where $W_x(a,\tau)$ are the wavelet coefficients and (*) denotes the complex conjugate form.

According to the mother wavelet, the frequency *f* can be substituted for the wavelet scale *a*. The wavelet power spectrum (*WPS*) is an estimation of the variance for the frequency *f* at the time position τ:

$$WPS_x(f,\tau) = |W_x(f,\tau)|^2$$

The wavelet cross spectrum *WCS* between *x*(*t*) and *y*(*t*) provides local information on the covariance at particular frequencies:

$$WCS_{x,y}(f,\tau) = W_x(f,\tau)W_y^*(f,\tau)$$

The clustering method consists of constructing a covariance matrix between each pair of WPS, and then to perform a Singular Value Decomposition, a technique also referred to as Maximum Covariance Analysis (MCA) (Bretherton *et al.*, 1992). The leading patterns and singular vectors obtained from this decomposition (the number of axes retained corresponds to a covariance threshold of 0.99) are compared in terms of distance according to the method developed by Rouyer *et al.* (2008a). Distances, based on the differences between each pair of leading pattern and singular vector, are ranked in a distance matrix; and a cluster analysis is carried out in order to represent a dendrogram.

Corbineau Ana, Rouyer T., Fromentin J.M., Cazelles B., Fonteneau Alain, Ménard Frédéric (2010)

Analysis of the spatial and temporal patterns of japanese tuna longline fisheries in the tropical world ocean

In : Proceedings of the fourth international symposium on GIS spatial analyses in fishery and aquatic sciences : vol. 4. Saitama : International Fishery GIS Society, 97-114

International Symposium on GIS-Spatial Analyses in Fishery and Aquatic Sciences , 4., Rio de Janeiro (BRA), 2008/08/25-29